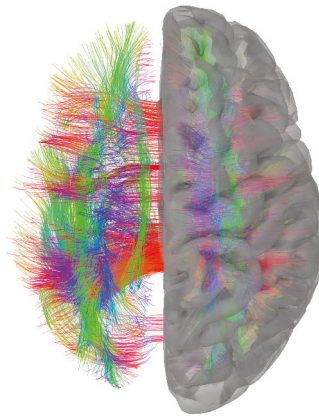


---

# Human brain dynamics during multitasking physical navigation

---

Tien-Thong Nguyen DO



Thesis: Doctor of Philosophy  
Faculty of Engineering and Information Technology  
University of Technology Sydney, Sydney, Australia (October 2020)

UNIVERSITY OF TECHNOLOGY SYDNEY  
Faculty of Engineering and Information Technology

**Human brain dynamics during multitasking  
physical navigation**

by

**Tien-Thong Nguyen DO**

THESIS SUBMITTED  
IN FULFILLMENT OF THE  
REQUIREMENTS FOR THE DEGREE OF

**Doctor of Philosophy**

Supervisors: Prof. Chin-Teng Lin  
Prof. Klaus Gramann  
Dr. Tim-Chen

Sydney, Australia

2020

# Certificate of Original Authorship

I, Tien-Thong Nguyen Do declare that this thesis, is submitted in fulfilment of the requirements for the award of Doctor of Philosophy, in the School of Computer Science, Faculty of Engineering and Information Technology at the University of Technology Sydney.

This thesis is wholly my own work unless otherwise referenced or acknowledged. In addition, I certify that all information sources and literature used are indicated in the thesis.

This document has not been submitted for qualifications at any other academic institution.

This research is supported by the Australian Government Research Training Program.

Production Note:

Signature: Signature removed prior to publication.

Date: 02 October 2020

© Copyright 2020 Tien-Thong Nguyen Do

# ABSTRACT

## **Human brain dynamics during multitasking physical navigation**

by

Tien-Thong Nguyen DO

Spatial navigation is an essential skill that helps one to keep track of their location and orientation and navigate efficiently through the environment. Investigating spatial cognitive processing can be beneficial by rendering a mechanism underlying diseases such as Alzheimer's disease, which might be diagnosed based on impairments in spatial tests long before established diagnostic criteria. Furthermore, navigation in real-life often involves multiple cognitive processes, such as landmark encoding, cognitive map anchoring, and goal-oriented planning, even in the simplest situation. Thus, investigating spatial navigation under multitasking situation might provide more insight of brain dynamics underlying navigation in our daily activities.

However, most studies on active physical navigation in 3D space are based on animal research, or the studies are confined to a specific patient population with limited movement ranges. These limitations hinder the generalization of findings in stationary laboratory set-ups to active navigation in healthy human participants.

In this work, we investigated human brain dynamics while multitasking in active navigation tasks in a more natural set-up that could be used with healthy populations. We performed simulated driving and physical spatial navigation task experiments, which mimic typical navigation tasks in our daily lives. Participants performed the tasks in a virtual environment, while their brain signal was measured simultaneously. We investigated brain dynamics of concurrent multitasking in the simulated driving experiment, where participants performed the driving task, and dynamic attention shifting task concurrently. We then further investigated brain dynamics in a physical spatial navigation experiment, where participants actively

ambulated from a location to several others.

We found an increase in the information flow of brain connectivity in the period of concurrent task response in the simulated driving experiment. Furthermore, in the same experiment, we observed an increase in frontal beta during the secondary task response. We then obtained a significant modulation of theta oscillations in the retrosplenial complex (RSC) during heading changes in the physical spatial navigation experiment; this is an essential mechanism for heading computation and generating the grid cell signal. Finally, we reported that local information processing in the RSC increases linearly with the navigation load level. The findings unpack the insight of brain dynamics and offer unprecedented benefits for estimating cognitive load in active navigation.

Dissertation directed by Professor Chin-Teng Lin  
Australian Artificial Intelligence Institute (AAIL)  
School of Computer Science  
University of Technology Sydney

To my loved ones

# Acknowledgments

A Ph.D. journey is challenging; it is up and down. To go through this journey, one needs to be persistent. Of course, the task cannot be finished without help and support from others.

Foremost, I would like to express my gratitude to my supervisors, Prof. Chin-Teng Lin, Prof. Klaus Gramann, and Dr. Tim Chen, for their endless support and patience. It is my great honor to be supervised by Prof. Chin-Teng Lin. He has inspired me in everything from fundamental science to advanced machine learning and neuroscience knowledge. Prof. Lin has always shared the vision for my long-term research to motivate me. I also want to thank Prof. Klaus Gramann (Technical University of Berlin) for supervising my spatial navigation study. He tirelessly guided me in the navigation research field, which is a new insight for me since the beginning of my studies. And Dr. Tim Chen (University of Adelaide) continuously helped me in the research pathway to reach my end goal. I would also like to express my appreciation to Prof. Tzyy-Ping Jung, a collaborator from the University of California San Diego (UCSD) for his time and effort in discussions on active navigation experiments.

Through my Ph.D. journey, I am fortunate to have worked with excellent colleagues from the Computational Intelligence and Brain-Computer Interfaces (CIBCI) lab, UTS. I want to thank Carlos Tirado, Avinash Singh, Howe Zhu, Khuong Tran, Ashlesha Akella, Alka John, Fred Chang, Jia Liu, Yurui Ming, Dr. Yukai Wang, and Dr. Mukesh Prasad. I would also like to thank my friends Anna Wunderlich and Tung Huynh for sharing scientific knowledge during my Ph.D. study.

I would like to thank the Australian Research Council (ARC) for its financial support. In addition, I want to extend my gratitude to the Research Training

Program (RTP) scheme from the Department of Education and Training for funding my stipend.

Lastly, I appreciate my parents, Do Dinh Qua and Nguyen Thi Thuy Tam, and my sister Do Thi Anh Dao, for their love and mental support. I would especially like to thank my wife, Hanh Duong, for your love, spirit, and endless support, understanding my Ph.D. journey in hardship and good times. This thesis could not have been finished without tremendous support from all of you.

Tien-Thong Nguyen Do  
Sydney, Australia, 2020.



## List of Publications

### Journal

- J-1. C.-L. Lin, and **T.-T.N. Do**, “Direct-Sense Brain–Computer Interfaces and Wearable Computers”. *IEEE Transactions on Systems, Man, and Cybernetics: Systems*, vol. 51, no. 1, pp. 298-312, 2021.
- J-2. **T.-T.N. Do**, Y.-K. Wang, and C.-T. Lin, “Increase in brain effective connectivity when workload increases but not with high fatigue,” *IEEE Transactions on Cognitive and Developmental Systems*, 2020.
- J-3. **T.-T.N. Do**, C.-H. Chuang, S.-J. Hsiao, C.-T. Lin, and Y.-K. Wang, “Neural comodulation of independent brain processes related to multitasking,” *IEEE Transactions on Neural Systems and Rehabilitation Engineering*, vol. 27, no. 6, pp. 1160-1169, 2019.
- J-4. **T.-T.N. Do**, C.-T. Lin, and K. Gramann, 2020, “Human retrosplenial theta and alpha modulation in active spatial navigation”. **(Under review)**
- J-5. **T.-T.N. Do**, T.-P. Jung, and C.-T. Lin, “Retrosplenial segregation reflects the navigation load during ambulatory movement”. **(Under review)**
- J-6. C. Cortes, H.-T. Chen, **T.-T.N. Do**, C.-T. Lin, “EEG Signals and Body Kinematics During Different Levels of VR Sickness”. **(Under review)**
- J-7. N.H.-Shariati, T. N.-John, A.K. Singh, C. Cortes, **T.-T.N. Do**, A. Craig, J.W. Middleton, M.P. Jensen, Z. Trost, C.-T. Lin, and S.M. Gustin, “Evaluation of the effectiveness of a novel brain-computer interface neuromodulative intervention to relieve neuropathic pain following spinal cord injury: protocol for a single-case experimental design with multiple baselines”, *JMIR Research Protocols*, vol. 9, no. 9, pp. e20979, 2020.

## Conference

- C-1. **T.-T.N. Do**, A.K. Singh, C. Cortes, and C.-T. Lin, “Estimating the cognitive load in physical spatial navigation” *IEEE Symposium Series on Computational Intelligence (SSCI)*, Canberra, Australia, pp. 568-575, Dec., 2020.
- C-2. **T.-T.N. Do**, C.-T. Lin, and K. Gramann, “Human brain dynamics during physical spatial navigation” *4th International Conference on Mobile Brain/Body Imaging (MoBI)*, San Diego, USA, Jun., 2020 (**Accepted**) (rescheduled to 2021 due to COVID pandemic).
- C-3. **T.-T.N. Do**, and T.T. Huynh, “Evaluate effects of multiple users in collaborative Brain-Computer Interfaces: A SSVEP study” *IEEE 8th International Conference on Communications and Electronics*, Phu Quoc, Vietnam, Jan., 2021 (**Accepted**) (rescheduled to 2021 due to COVID pandemic).
- C-4. **T.-T.N. Do**, C.-T. Lin, C. Cortes, A.K. Singh, J. Liu, H.-T. Chen, and K. Gramann, “Human brain dynamics during navigation with natural walking under different workload conditions in Virtual Reality (VR)” *Society for Neuroscience (SfN)*, Chicago, USA, Oct., 2019.
- C-5. J. Lu, A. Wunderlich, A.K. Singh, **T.-T.N. Do**, K. Gramann, and C.-T. Lin, “Investigating the impact of landmarks on spatial learning during active navigation” *Society for Neuroscience (SfN)*, Chicago, USA, Oct., 2019.

# Contents

Certificate	ii
Abstract	iii
Dedication	v
Acknowledgments	vi
List of Publications	viii
List of Figures	xv
List of Tables	xxvii
Abbreviation	xxviii
<b>1 Introduction</b>	<b>1</b>
1.1 Background . . . . .	1
1.1.1 The evidence of cognitive map in navigation . . . . .	1
1.1.2 Mechanism of cognitive map . . . . .	3
1.1.3 Navigation strategies - Spatial reference frame . . . . .	6
1.1.4 Multiple resource theory . . . . .	7
1.1.5 Limitations of brain imaging in navigation studies . . . . .	9
1.2 Research Problems . . . . .	11
1.2.1 Brain dynamics of concurrent multitasking . . . . .	11
1.2.2 The effect of fatigue on brain connectivity in multitasking . .	11
1.2.3 Heading computation in active navigation . . . . .	12

1.2.4	Local information processing in RSC under different navigation load conditions . . . . .	13
1.3	Thesis Organization . . . . .	13
<b>2</b>	<b>Techniques for Data Analysis</b>	<b>16</b>
2.1	Background . . . . .	16
2.2	Independent Component Analysis . . . . .	17
2.3	Source localization for inverted problem . . . . .	18
2.3.1	Single and multiple dipole fitting . . . . .	20
2.3.2	Distributed source modeling . . . . .	20
2.4	Group study . . . . .	21
2.4.1	Clustering: k-means . . . . .	22
2.4.2	Clustering: Repeated k-means . . . . .	22
<b>3</b>	<b>Brain dynamics in the concurrent multitasking</b>	<b>26</b>
3.1	Abstract . . . . .	26
3.2	Introduction . . . . .	27
3.3	Materials and Methods . . . . .	30
3.3.1	Participants . . . . .	30
3.3.2	Fatigue state . . . . .	31
3.3.3	Experiment paradigm . . . . .	32
3.3.4	Data acquisition . . . . .	33
3.3.5	Data Processing and Analysis . . . . .	34
3.4	Neural comodulation analysis . . . . .	35
3.5	Results of the comparison between single-task ad multiple-task conditions . . . . .	38

3.5.1	Behavioral Performance . . . . .	38
3.5.2	Event-Related Spectral Perturbation . . . . .	39
3.5.3	Independent Modulators and Their Activation . . . . .	41
3.6	Discussion . . . . .	45
3.6.1	Behavioral Performance during Distracted Driving . . . . .	45
3.6.2	EEG Correlates of Distracted Driving . . . . .	46
3.6.3	EEG Comodulatory Activity Correlates of Distracted Driving . . . . .	47
3.6.4	Potential Neurophysiological Mechanisms . . . . .	47
3.6.5	Possible Neural Modulation Mechanisms . . . . .	49
<b>4</b>	<b>The effect of fatigue on brain connectivity in multitasking</b>	<b>50</b>
4.1	Abstract . . . . .	50
4.2	Introduction . . . . .	51
4.3	Related works . . . . .	53
4.4	Materials and methods . . . . .	54
4.4.1	Experimental Design . . . . .	54
4.4.2	EEG data processing . . . . .	54
4.4.3	Effective connectivity . . . . .	56
4.5	Results . . . . .	58
4.5.1	Behavioral Performance . . . . .	58
4.5.2	Comparisons of ECs between single- and dual-task conditions in different fatigue states . . . . .	59
4.6	Discussion . . . . .	64
<b>5</b>	<b>Heading computation in active navigation</b>	<b>69</b>

5.1	Abstract . . . . .	69
5.2	Introduction . . . . .	69
5.3	Materials and Methods . . . . .	72
5.3.1	Participants . . . . .	72
5.3.2	Experiment design and tasks . . . . .	72
5.3.3	EEG analysis . . . . .	77
5.4	Results . . . . .	79
5.4.1	Behavior . . . . .	79
5.4.2	Event-related Spectral Perturbation (ERSP) . . . . .	80
5.4.3	Neural Correlations with Spatial Updating . . . . .	80
5.5	Discussion . . . . .	82
<b>6</b>	<b>Local information processing in RSC under different navigation load conditions</b>	<b>93</b>
6.1	Abstract . . . . .	93
6.2	Introduction . . . . .	93
6.3	Materials and Methods . . . . .	96
6.3.1	Experimental Design . . . . .	96
6.3.2	EEG analysis . . . . .	96
6.3.3	Functional connectivity . . . . .	98
6.3.4	Network properties . . . . .	99
6.4	Results . . . . .	100
6.4.1	Behavioral performance . . . . .	100
6.4.2	Functional connectivity . . . . .	100
6.5	Discussion . . . . .	103

## 7 Conclusion and Future Work 110

# List of Figures

1.1	Map- and grid-like coding of navigable space in humans. (a) Evidence from fMRI adaptation. When viewing images of landmarks from a familiar college campus, fMRI activity in the left hippocampus (Hipp) scales with the real-world distance between the landmark shown on each trial and the landmark shown on the immediately preceding trial. (b) Evidence from multi-voxel pattern analysis (MVPA). Voxelwise activity patterns in the hippocampus reflect distances between events intermittently logged by a camera worn by participants in the 30 days before the scan (aerial map of navigated territory shown on the left, as well as example pictures. (c) Evidence from an encoding model. Participants performed a navigation task in virtual reality. Grid cells in an individual rat all have the same orientation ( $\Phi$ ; top row), and thus it was predicted that movements aligned with the grid orientation should result in more fMRI activity than movements misaligned with the grid. The expected pattern of results was observed in the human entorhinal cortex (EC, bottom row). Reprinted by permission from Springer Nature, Nature Neuroscience, Epstein et al. (2017) ©.	4
1.2	Cortical areas involved in spatial reference frame processing/visual perspective-taking. Based on data from a meta-analytic study of Arora et al. (2015), and the studies of Burgess et al. (2001) and Committeri et al. (2004). Reprinted from NeuroImage, vol 161, Vukovic and Shtyrov, Cortical networks for reference-frame processing are shared by language and spatial navigation systems, pages 120-133, ©2020, with permission from Elsevier	5



1.3	The key anatomical and functional relationships of the retrosplenial cortex. Effective episodic memory, navigation and future thinking all require the ability to integrate and manipulate different frameworks of information, for example egocentric (self-centered) and allocentric (world-centered) frameworks. By virtue of its principal connections, the retrosplenial cortex is uniquely placed to enable translation within these domains: ATN, anterior thalamic nuclei. Reprinted by permission from Springer Nature, Nature Reviews Neuroscience, Vann et al. (2009) ©. . . .	10
1.4	Research map in this thesis. . . . .	15
2.1	The set-up of the EEG experiment. (a) The EEG cap. (b) The EEG channel location with the scalp template. (c) The distributed source of activation in the brain cortex. . . . .	18
2.2	The results of the ICA solution. The largest 18 independent components from a participant in a physical navigation study. . . . .	19
2.3	The dipole fitting solution. (a) The first ten largest independent component dipoles location projected on the MRI template. Each dipole (coded by color) represents location and orientation. (b) The dipole locations projected on the scalp map. The number on the top indicates the IC number and its corresponding residual variance (RV). . . . .	20
2.4	The distributed source localization solution. The cortex source activity (right hemisphere) of a participant in the first 600 ms in the physical navigation study (chapter 5, and 6). . . . .	21

2.5	Clustering solution. The color indicates different cluster regions: yellow, green, blue, red, pink, and white indicate frontal, sensorimotor, parietal, retrosplenial complex, occipital, and muscle, respectively. Small sphere indicates an independent component; the large sphere indicates the cluster centroid of the cluster. Figure adapted from the results of the physical navigation experiment in Chapter 5. . . . .	23
2.6	Evaluation of multivariance from 10,000 times clustering based on the score of each cluster solution, including: (i) the number of participants; (ii) the ratio of the number of ICs per participant; (iii) the cluster spreading (mean squared distance of each IC to the cluster centroid); (iv) the mean RV of the fitted dipoles; (v) the distance of the cluster centroid to the ROI; and (vi) the Mahalanobis distance to the median distribution of the solutions. . .	24
2.7	Clustering solution for the retrosplenial complex cluster - top eight highest ranked solutions with grand scalp map and dipole location. .	25
3.1	a, Effectiveness score (ES) distributions. One dot indicates one dataset. (i), normal fatigue group (white), (ii) reduced fatigue group (light pinks) and (iii) high-risk fatigue group (light purple). b, Effectiveness score (ES) distributions between task and fatigue groups after the model validation test for effectiveness connectivity (EC) estimations. . . . .	31
3.2	Experimental design. (a) Virtually simulated environment for the driving task. (b) Two buttons were placed on the wheel for the DAS task response. (c) Experimental design; case 1: Lane-keeping task (LKT) only; case 2: concurrent LKT and visual dynamic attention shift ( $DAS_V$ ) dual tasks; case 3: concurrent LKT and auditory dynamic attention shift ( $DAS_A$ ) dual tasks. . . . .	32

3.3	The behavioral performance among the single- and dual-task conditions. The averaged driving response time of LKT (gray bar), $DAS_V$ (yellow bar) and $DAS_A$ (green bar) in each condition are listed. The averaged driving response time were significant different among three cases ( $p < 0.05$ ). . . . .	39
3.4	The Event-Related Brain Dynamics in three cases (rows) across brain regions (column), including the frontal, central, parietal, occipital, and temporal components (top). a) The ERSP in the Case 1 (LKT). b) The ERSP in the Case 2 ( $DAS_V$ ). c) The ERSP in the Case 3 ( $DAS_A$ ). The black-vertical line indicates stimulus onset (deviation onset), the blue-vertical line indicates driving response, and the red-vertical line indicates DAS response. . . . .	40
3.5	The event-relative independent modulator activation. a) The performance- related IM activation changes in LKT, $DAS_V$ , and $DAS_A$ conditions. b) The event-related IM activation changes in LKT, $DAS_V$ , and $DAS_A$ conditions. c) The IM activation difference among different conditions. The first column showed the difference between Case 1 (grey curve) and Case 2 (yellow curve). The second column showed the difference between Case 1 (grey curve) and Case 3 (green curve). The last column showed the difference between Case 2 (yellow curve) and Case 3 (green curve). The IM activation difference is significant at the 0.05 level (blue *). . . . .	43
3.6	The relative weight from IMs to each frequency band of ICs. Each column represents the relative weight of projection from the IM (the top row) to each frequency band (delta, theta, alpha, beta, and gamma band) of each selected IC (the leftmost column). For each IM, the red bar plots the significant difference among each frequency band of each selected IC. .	44
4.1	Flowchart of effective connectivity estimation. . . . .	55

4.2	EEG channels selected for estimating effective connectivity. . . . .	56
4.3	Reaction time and effectiveness score. Reaction time of lane-keeping task (LKT) across three tasks in three fatigue groups. The RTs of the LKT significantly increase in the high-risk state ( $p < 0.05$ ). There is no significant difference among the fatigue states when performing the $DAS_V$ and $DAS_A$ . . . . .	59
4.4	Topographical comparisons of significant EEG effective connectivity differences ( $p < 0.05$ ) between task conditions. The first column shows a comparison between the concurrent dual-task $DAS_V$ and LKT (V), the second column shows a comparison between the concurrent dual-task $DAS_A$ and LKT (A), and the third column shows a comparison between the concurrent dual-task $DAS_A$ and $DAS_V$ (AV). Line colors indicate the differences in connectivity strength between electrode pairs, with red indicating positive differences (more information flow) and blue indicating negative differences (less information flow). The directions of the arrows represent the direct paths of inter-channel information flow. . .	64
4.5	Topographical comparisons of significant EEG effective connectivity differences ( $p < 0.01$ ) between task conditions in each fatigue group. (a) Normal. (b) Reduced. (c) High-risk. The first column shows a comparison between the concurrent dual-task $DAS_V$ and LKT (V), the second column shows a comparison between the concurrent dual-task $DAS_A$ and LKT (A), and the third column shows a comparison between the concurrent dual-task $DAS_A$ and $DAS_V$ (AV). Line colors indicate the differences in connectivity strength between electrode pairs, with red indicating positive differences (more information flow) and blue indicating negative differences (less information flow). The directions of the arrows represent the direct paths of inter-channel information flow (note: V case used $p < 0.05$ ). . . . .	65

4.6	Number of significantly different brain connectivity edges between the dual- and single-task conditions across brain networks ( $p < 0.05$ ) in delta, theta, alpha and beta bands. The green background indicates the normal fatigue group, the light green background indicates the reduced fatigue group, the light red background indicates the high-risk fatigue group and the blue background indicates the dual- vs single-task without considering the fatigue state. The number indicates the number of brain connectivity edge significant differences ( $p < 0.05$ ). The light red/blue bar indicates the number of significant edge increase/decrease differences in the concurrent dual-task $DAS_V$ vs single-task LKT comparison. The dark red/blue bar indicates the number of significant edge increase/decrease differences in the comparison of the concurrent dual-task $DAS_A$ vs single-task LKT. . . . .	67
-----	--	----

- 5.1 Depiction of a passage through a tunnel with a turn to the right, with nonparallel start and end segments. The left-side displays a nonturner (dark grey head representing the perceived heading and the small light grey head representing the cognitive heading) using an allocentric frame of reference, with the navigator's heading during the first segment (a), during the turn (b), and during the last segment (c) of the tunnel passage. Note that the perceived and the cognitive heading diverge during the turn. On the right, a turner (light grey head representing the perceived cognitive heading which is assumed to be identical to the cognitive heading) is displayed who uses an egocentric frame of reference. During the first segment (a), the turner's heading is the same as that of a nonturner. During the turn, the axis of orientation changes (b). At the end of the tunnel, the turner's cognitive heading is different from that of a nonturner. Note that turners build up an additional allocentric frame of reference if they are forced to react based on an allocentric frame. There is no depiction of an additional allocentric reference frame for turners to emphasize the preferred use of an egocentric frame of reference by this strategy group. To the right-side of the figure, examples of homing vectors are displayed with the correct angular adjustment for a tunnel with one turn of  $60^\circ$  to the right, with panel D depicting the correct homing vector for nonturners, and panel E that for turners. Reprinted from Brain Research, Vol 1118, K. Gramann, H.J. Müller, B. Schönebeck, G. Debus, The neural basis of ego- and allocentric reference frames in spatial navigation: Evidence from spatio-temporal coupled current density reconstruction, Pages No. 116-129, Copyright (2021), with permission from Elsevier. . . . . 73

5.2	Experiment Design. a. Trial representation. At beginning of the trial, participant had 4 seconds to remember a landmark position which appeared in front of them (around 200 meters). Then participant performed navigation in walk1x and walk2x with random 2 or 3 turns within each walk. In the middle of the trial, participant performed the letter encoding task with random of 3, or 5, or 7 letters. The green squares indicated for the spatial retrieval task, while red squares indicated for the letter retrieval task. b. There were 20 turning points (4 walking paths, path 1 - point <sub>0.1.2.3.4.5</sub> , path 2 - point <sub>5.6.7.8.9.10</sub> ), path 3 - point <sub>10.11.12.13.14.15</sub> and path 4 - point <sub>15.16.17.18.19.20</sub> ) in this experiment. The red dots indicated for the turning points. The reference frame proclivity test (RFPT) was based on the participant response in path 3 at dot number 12, the participant was considered using egocentric or allocentric if their response was left or right arrow respectively. . . . .	74
5.3	The pipeline of EEG preprocessing. . . . .	86
5.4	The ERSP before and after noise removal. The RSP ERSP before and after noise removal at the participant level. The left figure shows the average ERSP for participants before noise removal. The right figure shows the average ERSP for participants after noise removal at: (a) one egocentric participant; and (b) one allocentric participant. . . . .	86
5.5	ERSP in several brain regions. The ERSP in different brain regions in or near the RSC (red), parietal cortex (blue), occipital cortex (pink), and neck (white). . . . .	87
5.6	Effective brain connectivity. The estimated effective connectivity of the four clusters (the RSC, neck, near the ear on the left side, and near the ear on the right side) in one participant in the (a) allocentric and (b) egocentric strategy groups. The results indicate that theta activity in the neck cluster has no effect on the RSC. . . .	87

5.7	The permutation test (n=2000, FDR-correlated) of the RSC ERSP for 6 segments in comparison to segment 1. . . . .	88
5.8	Correlation between landmark pointing error and ERSP at participant level. These are correlation coefficients between performance and the RSC ERSP in the continuous frequency (3-45 Hz) in the first ten percent (left column) and middle ten percent (right column) of the segment length. The asterisk (*) indicates a significant difference (p<0.05) between the allocentric (red) and egocentric strategies (blue). . . . .	89
5.9	The results of participant behaviour. a. The participant behaviour in the landmark pointing task. The X axis indicated for the number of turn points in the trial, the Y axis indicated for the absolute error of participant when they performed the landmark pointing task (the error was measured by the angular difference between the pointing vector and the participant to landmark vector). The regression was visualized by the red line (*, **, ***, **** indicated for p<.05, p<.01, p<.001, p<.0001 respectively). b. The RFPT results were in both passive condition (stationary test with the tunnel paradigm) and active condition (based on the participant's response at position 12, path 3 in the Figure 1b). Three groups of strategies egocentric, mixed and allocentric were colour coded with green, blue and red, respectively. . . . .	90
5.10	Retrosplenial complex (RSC) event-related spectral perturbation (ERSP). a. Dipole locations of independent component ( in or near retrosplenial complex (RSC) cluster at the sagittal, coronal, and top view respectively and the corresponding mean of scalp map. b. The RSC ERSP with respect to segment of turns from 1 to 6 turns. c. The permutation test (n=2000, FDR-correlated) of the RSC ERSP in 6 segments. . . . .	91



5.11 RSC ERSP correlated with participant performance in the first 10 percent (a) and mid 10 percent (b) of the segment length in both participant and trial level respectively. The top figure showed the correlation coefficients computed (the number on the bottom right corner, red color indicated for statistical significance; \*, \*\*, \*\*\*, \*\*\*\* indicated for  $p < .05$ ,  $p < .01$ ,  $p < .001$ ,  $p < .0001$  respectively) between individual performance and RSC ERSP at participant level in different frequency band at theta (4-8 Hz), low Alpha (8-10 Hz), high Alpha (10-12 Hz), and beta (12-30 Hz). The row indicated for the RFP strategy in the passive RFPT response: the red colour indicates for allocentric, and blue indicates for egocentric strategy. The bottom figure showed the correlation coefficients computed between individual performance and RSC ERSP in the trial level at same the range of frequency as top figure. The color-coded indicated for RFP strategy; the lighter color in the same RFP strategy group indicated for active allocentric response, while the darker color indicated for active egocentric trial response. . . . . 92

6.1	The experimental design. (a) Trial representation. At the beginning of the trial, participants had 4 seconds to remember a landmark, which was presented approximately 200 meters in front of them. Then, the landmark disappeared (in the rest of the trial), and participants answered the question: “Where is the landmark position?” (Resp. 1, green square). Next, participants freely walked in a predefined path with the number of turns points being randomly chosen as 2 or 3 (walk 1x). Subsequently, participants were asked to recall the landmark position (Resp. 2, green square). Next, participants encoded a set of letters (3, 5, or 7 letters) (orange square) and then performed the letter-retrieval task (Resp. 3, red square). Then, participants started the second walk (2x) with 2 or 3 turn points. After finishing the walk, participants performed the letter-retrieval task (Resp. 4, red square) and spatial-retrieval task (Resp. 5, green square). (b) EEG cap set up. (c) The participant responded to a landmark position. . . . .	97
6.2	pipeline for brain network segregation and integration analysis. . . .	98
6.3	The landmark-pointing response error (absolute) across walking segments with a distinct NT during the navigation trial. The Wilcoxon signed-rank tests were used to check for significant differences between behavior performance (*, **, ***, and **** indicate $p < 0.05$ , $p < 0.01$ , $p < 0.001$ , and $p < 0.0001$ , respectively) . . . .	102
6.4	Functional connectivity of the brain network across six walking segments in the (a) theta band and (b) alpha band. The nodes indicate brain regions (based on 68 Desikan-Killiany atlas). The edges indicate a significant connection between nodes; the edge size indicates the strength of the connection. . . . .	103

6.5 Graph properties at the frontal and retrosplenial complex (RSC):  
    (a) Clustering coefficient (a) and (b) participation coefficient across  
    six walking segments in various frequency ranges. Pairwise post hoc  
    Wilcoxon signed-rank tests (FDR-corrected) were used to check for  
    significant differences between walking segments (\* and \*\* indicate  
     $p < 0.05$  and  $p < 0.01$ , respectively). . . . . 106

6.6 Network atlas. . . . . 107

6.7 Clustering coefficient among different brain networks, including the  
    whole-brain network, frontoparietal network, somatosensory  
    network, visual network, and default mode network across walking  
    segments under various frequencies. . . . . 108

6.8 Participation coefficients among different brain networks, including  
    the whole-brain network, frontoparietal network, somatosensory  
    network, visual network, and default mode network, across walking  
    segments under various frequencies. . . . . 109

## List of Tables

4.1	Brain areas and respective EEG channels selected for estimating effective connectivity. . . . .	57
4.2	Validation results of effective connectivity model estimation. . . . .	63
6.1	Error in the landmark pointing task. The first and second columns indicate the number of turning points, the third column contains the p-values (FDR-adjusted) of the Wilcoxon signed-rank tests (the *, **, ***, and **** indicate for $p < .05$ , $p < .01$ , $p < .001$ , and $p < .0001$ , respectively. . . . .	101

# Abbreviation

EEG - Electroencephalography

MEG - Magnetoencephalogram

fMRI - functional Magnetic Resonance Imaging

ERSP - Event-Related Spectral Perturbation

ICA - Independent Component Analysis

AMICA - Adaptive Mixture Independent Component Analysis

PCA - Principle Component Analysis

sLORETA - standardized Low-Resolution Brain Electromagnetic Tomography

PLV - Phase Locking Value

MoBI - Mobile Brain/Body Imaging

RFP - Reference Frame Proclivity

HD - Head Direction

FM $\theta$  - Frontal Midline Theta

SAFTE - Sleep, Activity, Fatigue, and Task Effectiveness